L-Histidine tetrafluoroborate: a solution-grown semiorganic crystal for nonlinear frequency conversion

H. O. Marcy, M. J. Rosker, L. F. Warren, P. H. Cunningham, and C. A. Thomas

Rockwell International Science Center, 1049 Camono Dos Rios, Thousand Oaks, California 91360

L. A. DeLoach, S. P. Velsko, and C. A. Ebbers

Lawrence Livermore National Laboratory, P.O. Box 808, L-250, Livermore, California 94550

J.-H. Liao and M. G. Kanatzidis

Department of Chemistry, Michigan State University, East Lansing, Michigan 48824

Received June 20, 1994

The crystal structure, refractive indices, and phase-matching conditions for a new nonlinear optical material, L-histidine tetrafluoroborate (HFB), are reported. HFB grows readily, displays favorable mechanical characteristics, and has adequate birefringence to permit phase-matched parametric processes over much of its transparency range (250 nm to 1300 nm). The phase-matching loci and angular sensitivity for second-harmonic generation of 1064-nm light in single crystals of HFB were measured. The effective nonlinearity for HFB is comparable with that of β-barium borate ($\sim$2 pm/V), and its angular sensitivity $[\delta(\Delta k)/\delta\theta]$ is somewhat smaller.

Advanced laser-based imaging, communication, data storage, and countermeasure system designs require improved nonlinear optical (NLO) materials. In particular, there are identifiable systems applications for lower-cost, higher-response, higher-average-power NLO materials for optical parametric amplifier operation and second-harmonic generation (SHG) throughout the blue/near-UV spectral region. We report here preliminary results for a new and promising solution-grown NLO material, L-histidine tetrafluoroborate $\{[(C_3N_2H_4)CH_2CH(NH_3)(CO_2)]^+BF_4^-$; HFB$\}$.

HFB is an example of a semiorganic NLO material, in which the high optical nonlinearity of a purely organic material is combined with the favorable mechanical and thermal properties of an inorganic.[1,2] Much recent work[3,4] has demonstrated that organic crystals can have very large nonlinear susceptibilities compared with inorganic crystals, but their use is impeded by their low optical transparencies, poor mechanical properties, low laser damage thresholds, and an inability to produce and process large crystals. Purely inorganic NLO materials typically have excellent mechanical and thermal properties but possess relatively modest optical nonlinearities because of the lack of extended π-electron delocalization. In semiorganics, polarizable organic molecules are stoichiometrically bound within an inorganic host, e.g., an organic ion/inorganic counterion salt, such as L-arginine phosphate,[5] or an organic ligand/metal ion complex, such as zinc tris(thiourea) sulfate.[1] Imparting ionic character to large NLO response organic molecules by complexation and/or salt formation improves the mechanical and optical properties of the crystals of these materials and provides a high degree of design flexibility for NLO effects by use of simple synthesis and screening techniques. HFB was identified as a potentially useful NLO material in our ongoing survey of semiorganic materials for applications requiring large-aperture, high-average-power frequency conversion in the visible and the near IR.

We prepared HFB by dissolving one equivalent of L-histidine in water containing one equivalent of tetrafluoroboric acid, whereupon ambient temperature solvent evaporation led to the separation of rodlike crystals. Single crystals were obtained from recrystallized material by slow evaporation from water. HFB crystallizes in the monoclinic space group $P2_1$ [$a = 0.5022(2)$ nm, $b = 0.9090(1)$ nm, $c = 1.0216(2)$ nm, $\beta = 93.484(8)°$]. We determined the HFB crystal structure at 23 °C by using a single-crystal diffractometer and the intensities of 4754 reflections probed with Cu Kα radiation. Crystals belonging to symmetry class 2 have eight nonzero d-coefficient tensor components, allowing for the possibility of significant on- and off-axis nonlinear coupling. A projection of the crystal structure (Fig. 1) showed significant orientation of the five-membered imidazole ring $(C_3N_2H_4)^+$ planes along the a axis. The imidazole and amino $(NH_3)^+$ groups are protonated and thus counterbalance the negative charges of the carboxylate $(CO_2)^-$ functionality and the tetrafluoroborate $(BF_4)^-$ ion. We presume that the principal optical nonlinearities of HFB arise from delocalized π electrons associated with the histidine imidazolium and carboxylate functionalities. UV–visible transmission measurements on single crystals of HFB showed that it is optically transparent between 250 and 1300 nm. The UV absorption edge is probably defined by the electronic absorption associated with the imidazole group. Thermogravimetric analysis shows that HFB has a decomposition

0146-9592/95/030252-03$6.00/0

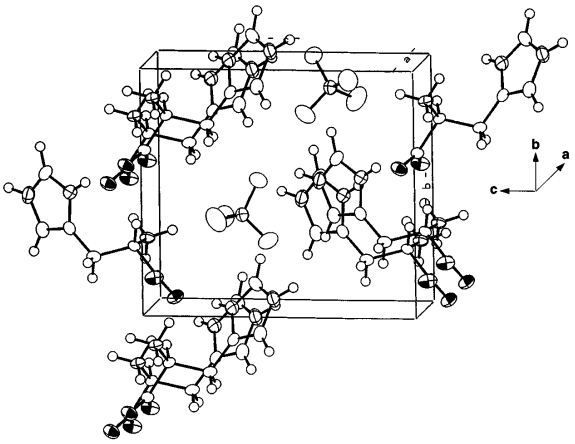

Fig. 1. Unit formula and a projection of the crystal structure for HFB.

temperature of 205 °C. Exposure of the crystal surfaces to humid and dry atmospheres indicates that HFB is stable and nonhygroscopic.

The refractive indices for HFB were measured using the spindle stage refractometer technique[6] at 10 wavelengths between 365 and 1050 nm on small (e.g., 50- to 200-μm) single-crystal fragments. This technique uses optical crystallographic methods to orient a crystal on a microscope spindle stage and then match its refractive index to that of an immersion fluid. The data were fitted to a single-pole Sellmeier equation:

$$n_i^2 = a_i + \frac{b_i}{\lambda^2 - c_i} - d_i\lambda^2, \qquad i = \alpha, \beta, \gamma, \qquad (1)$$

where the assignment $n_\alpha < n_\beta < n_\gamma$ has been made. The following results were obtained: $a_\alpha = 2.1415$, $b_\alpha = 0.01536$, $c_\alpha = 0.022437$, $d_\alpha = 0.0085411$; $a_\beta = 2.3281$, $b_\beta = 0.015229$, $c_\beta = 0.023190$, $d_\beta = 0.0083626$; $a_\gamma = 2.4474$, $b_\gamma = 0.014216$, $c_\gamma = 0.035942$, $d_\gamma = 0.021689$. The difference between data and fit was less than ± 0.0005. Calculations based on these fits indicate that HFB has sufficient birefringence to phase match for parametric processes between 300 and 1300 nm, including SHG of 1064-nm light and sum-frequency mixing of 1064 and 532 nm to produce 355-nm light. We are currently growing large crystals to cut oriented prisms for unambiguously identifying the crystallographic directions with the principal refractive indices.

The measured Type I and Type II 1064-nm SHG phase-matching (PM) loci for HFB are shown relative to the principal dielectric axes in the Wulf net projection[7] of Fig. 2. These data were measured on ~1-mm diameter spheres of HFB with a computer-automated version of the direct phase-matching technique described in Ref. 8. This method makes use of optical crystallographic techniques to grind and mount a single-crystal sphere on a goniometer. Laser light was then used to locate all crystal orientations phase matched for SHG (i.e., the PM locus). Such PM crystal orientations can be identified by their strong SHG signal with a sinc^2 angular dependence along lines perpendicular to the PM locus.

Beginning with two manually determined PM orientations, the entire PM locus was discovered by our computer-controlled acquisition as follows. Using the determined PM orientations, we made an estimate of the next point along the locus and calculated a set of orientations along the line perpendicular to the locus at this point. The intensity of the SHG was measured for these orientations and fitted to the function $I_{2\omega} = A\ \mathrm{sinc}^2[\frac{1}{2}\beta(\eta - \eta_0)L]$, where η is the angle along the perpendicular and L is the crystal length. The fit parameters A, β and η_0 gave estimates of the amplitude, angular sensitivity, and position, respectively, of the next determined point on the locus. These fits were generally excellent. This process was repeated until the entire locus was mapped. After each determination we adjusted the polarization of the fundamental laser light to maintain the maximum amount of SHG signal for the particular PM process (Type I or Type II). In Figs. 2 and 3, $\theta = 0°$ and $\phi = 0°$ correspond to propagation along the dielectric axis having the smallest refractive index (n_α), and $\theta = \pm 90°$ and $\phi = 0°$ correspond to propagation along the dielectric axis having the highest refractive index (n_γ). The inherent symmetry of the coordinates for the PM loci permits angular transformation to the proper crystal frame after data acquisition in the laboratory frame.

The variation of the effective nonlinearity and the angular acceptance as a function of crystal orientation is more clearly depicted in Fig. 3. Figure 3(a) shows that the experimentally determined PM coordinates agree well with the values calculated using the Sellmeier fits. The observed variations in the effective nonlinearities [Fig. 3(c)] are consistent with those expected for a crystal having class 2 symmetry. Of particular interest is that the maximum Type I coupling occurs in the $\alpha - \gamma$ plane. This allows the possibility of large nonlinear coupling in an orientation with small angular sensitivity, $[\delta(\Delta k)/\delta\theta]$. This occurrence should cause HFB to have a low and therefor favorable threshold power figure of merit,[5] as discussed in more detail below.

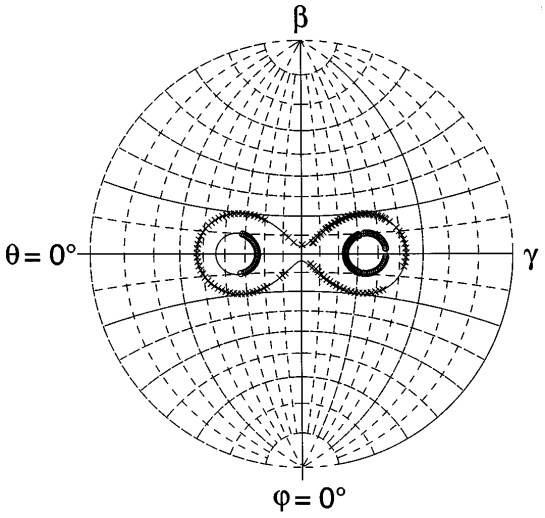

Fig. 2. Wulf net projection showing the measured and calculated phase-matching loci for HFB for Type I PM (circles) and Type II PM (crosses). The solid curves were calculated with Eq. (1).

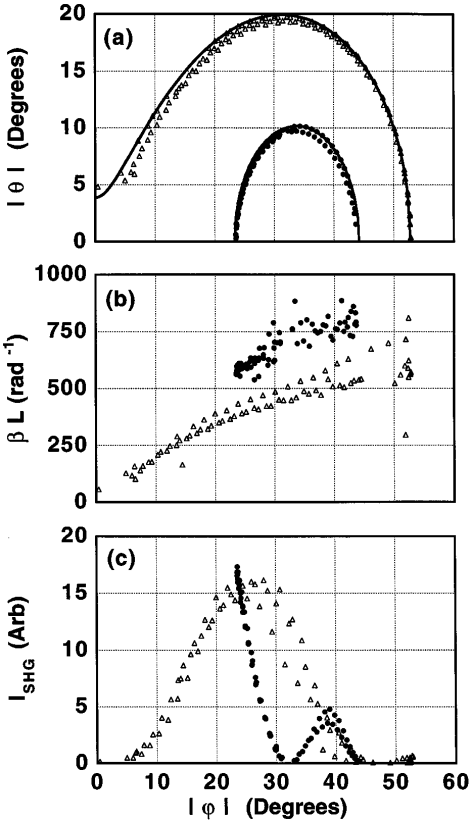

Fig. 3. Measurements of (a) the PM loci, (b) the angular sensitivities, and (c) the intensity dependences for HFB. Data are shown for Type I (circles) and Type II (triangles) from all four quandrants. The solid curves in (a) were calculated with Eq. (1).

We compared the maximum effective nonlinearities determined from the direct PM data obtained on a sphere of HFB [Fig. 3(c)] with those for a 0.5-mm plate of KDP, but for Type II PM, using the relation

$$d_{\mathrm{eff}}^{\mathrm{sample}} = \frac{n_{\omega}^{\mathrm{sample}}}{n_{\omega}^{\mathrm{KDP}}} \left(\frac{n_{2\omega}^{\mathrm{sample}} I_{2\omega}^{\mathrm{sample}}}{n_{2\omega}^{\mathrm{KDP}} I_{2\omega}^{\mathrm{KDP}}} \right)^{1/2} \left(\frac{L_{\mathrm{KDP}}}{L_{\mathrm{sample}}} \right) d_{\mathrm{eff}}^{\mathrm{KDP}}, \tag{2}$$

where L represents the crystal path length and $I_{2\omega}$ is the measured intensity of signal beam. This analysis indicated that at its maximum HFB has an effective nonlinearity of approximately five times that of the KDP standard ($d_{\mathrm{eff}}^{\mathrm{HFB}} \approx 2$ pm/V, assuming d_{36} of KDP = 0.39 pm/V). This value, however, should be taken only as a lower bound for d_{eff}; our experience has shown that the direct PM sphere data underestimate the value of the effective nonlinearity because of the relatively poor internal quality and surface polish typical for such small-sphere samples.

Figure 3(b) shows the estimate of the angular sensitivity for HFB, as determined by the data fits. For the orientations giving the maximum nonlinear signals, the angular sensitivities were approximately 5400 and 3800 (cm rad)$^{-1}$ for Type I and Type II PM, respectively. Although there is little variation in the acceptance angle for HFB with crystal orientation, it is important to note that the position of maximum nonlinearity for both the Type I and Type II loci occurs near a maximum in the acceptance angle. Although more-accurate determinations of d_{eff} and angular sensitivity $\delta(\Delta k)/\delta\theta$ on cut and polished plates of HFB will be necessary before firm conclusions can be drawn, preliminary analysis of these data indicates that HFB appears to be less angularly sensitive than β-barium borate (BBO) at its orientation of maximum coupling. Using the equation $P_{\mathrm{th}} = (\lambda\beta\theta/C)^2$, where P_{th} is the power threshold, λ is the wavelength of fundamental beam, β_{θ} is the angular sensitivity in (cm rad)$^{-1}$, and $C = 5.46 d_{\mathrm{eff}}/\lambda(n_1 n_2 n_3)^{1/2}$, with d_{eff} in pm/V and λ in μm,[5] we can estimate an upper bound for the power threshold figure of merit for HFB. This power threshold is the amount of power required in a diffraction-limited beam to achieve 50% conversion to the second harmonic; thus, the lower the value for P_{th}, the more practical the material. For Type II SHG in HFB, the power threshold estimated from these preliminary data is $\leq$6 MW, which compares favorably with that of KDP (P_{th} = 67 MW) and is between that of the high-temperature melt-grown materials BBO (P_{th} = 22.6 MW) and lithium triborate (LBO) (P_{th} = 0.42 MW).

These preliminary results suggest that HFB shows promise as a new NLO material for frequency conversion in the near UV to the near IR. The birefringence of HFB was found to be adequate to permit PM throughout its transmission range for common three-wave frequency conversion processes. By measuring the SHG obtained as a function of orientation of a small crystal, we have determined the nonlinearity to be at least five times that of KDP and have shown that the power threshold figure of merit should compare favorably with those of high-temperature, melt-grown materials, such as BBO and LBO. These results serve to further validate the semiorganic approach to developing solution-grown alternatives to these latter materials.

References

1. H. O. Marcy, L. F. Warren, M. S. Webb, C. A. Ebbers, S. P. Velsko, G. C. Kennedy, and C. C. Catella, Appl. Opt. **31,** 5051 (1992).
2. L. F. Warren, in *Electronic Materials—Our Future,* R. E. Allred, R. J. Martinez, and K. B. Wischmann, eds. (Society for the Advancement of Material and Process Engineering, Covina, Calif., 1990), pp. 388–396.
3. G. R. Meredith, in *Nonlinear Optical Properties of Organic and Polymeric Materials,* D. J. Williams, ed., ACS Symp. Ser. **233** (1982), pp. 27–56.
4. S. R. Marder, J. E. Sohn, and G. D. Stucky, eds., *Materials for Nonlinear Optics—Chemical Perspectives,* ACS Symp. Ser. **455** (1991).
5. D. Eimerl, IEEE J. Quantum Electron. **QE-23,** 575 (1987).
6. L. E. Davis, Proc. Soc. Photo-Opt. Instrum. Eng. 133 (1987).
7. F. D. Bloss, in *An Introduction to the Methods of Optical Crystallography* (Holt, Rinehart & Winston, New York, 1961), Chap. 9.
8. S. P. Velsko, Opt. Eng. **28,** 76 (1989).